

## Characterization of Poly(ethylene oxide)-*b*-Poly(L-lactide) Block Copolymer by Matrix-Assisted Laser Desorption/Ionization Time-of-Flight Mass Spectrometry

Jeongmin Hong, Donghyun Cho, and Taihyun Chang\*

*Department of Chemistry and Center for Integrated Molecular Systems,  
Pohang University of Science and Technology, Pohang 790-784, Korea*

Woo Sun Shim and Doo Sung Lee

*Department of Polymer Science and Engineering, Sungkyunkwan University, Suwon 440-746, Korea*

*Received Apr. 30, 2003; Revised July 21, 2003*

**Abstract:** A poly(ethylene oxide)-*b*-poly(L-lactide) diblock copolymer (PEO-*b*-PLLA) is characterized by matrix-assisted laser desorption/ionization time-of-flight mass spectrometry (MALDI-TOF MS) and a block length distribution map is constructed. Although the MALDI-TOF mass spectrum of PEO-*b*-PLLA is very complicated, most of the polymer species were identified by isolating the overlapped isotope patterns and by fitting the overlapped peaks to the Schulz-Zimm distribution function. Reconstructed MALDI-TOF MS spectrum was nearly identical to the measured spectrum and this method shows its potential to be developed as an easy and fast analysis method of low molecular weight block copolymers.

**Keywords:** PEO-*b*-PLLA, block copolymer, MALDI-TOF MS, isotope, molecular weight distribution.

### Introduction

Poly(ethylene oxide)-*block*-poly(L-lactide) (PEO-*b*-PLLA), a nonionic water-soluble block copolymer with a hydrophilic PEO component and a hydrophobic PLLA component, has attracted much attention in the field of pharmaceutical and biomedical applications due to its biodegradability and biocompatibility.<sup>1-4</sup> Various physical properties, such as sol-gel transition, micellization, and degradation, depend on the composition and chain architecture. In particular, the balance of hydrophilic and hydrophobic components is a crucial factor in controlling various physical properties.<sup>1,2</sup> Consequently, the accurate molecular weight characterization of the individual block length of the block copolymer is highly desired.

The precise characterization of a copolymer having both molecular weight distribution (MWD) and chemical composition distribution (CCD) is much more complicated than the analysis of a homopolymer. The ultimate goal would be the construction of a two-dimensional distribution map, one in molecular weight and the other in chemical composition, if there exist only the two distributions. The most popular method for this purpose is the two dimensional liquid chro-

matography (2D-LC), in which two different chromatographic separation methods are used in sequence.<sup>5-7</sup> If one of the two separation methods is sensitive to one molecular characteristic while not to the other, and vice versa, it would be possible to construct such a 2D distribution map. This method has been proven to be useful for the characterization of a copolymer having wide CCD and MWD. Also the approach has been used efficiently to characterize low molecular weight diblock copolymers.<sup>8-10</sup>

Another approach is the liquid chromatography at the chromatographic critical condition (LCCC).<sup>6,11</sup> At the LCCC condition of a homopolymer, the entropic size exclusion effect and the enthalpic interaction effect compensate each other, and the molecular weight dependence of the chromatography retention disappears. Therefore, at the LCCC condition of a block for a block copolymer, the block becomes "chromatographically invisible" and the other "visible" block solely determines the chromatography retention of the block copolymer. If the MWD of each block were characterized in this manner, the information equivalent to 2D map of MWD and CCD can be obtained. The other promising technique is the combination of liquid chromatography and mass spectrometry for the characterization of block copolymers. Recently the matrix-assisted laser desorption/ionization time-of-flight (MALDI-TOF) mass spectrometry has become a powerful tool for polymer characterization by virtue of the

\*e-mail : tc@postech.edu

1598-5032/10/341-06©2003 Polymer Society of Korea

soft ionization characteristic that produces mainly single-charged quasi-molecular ions with little fragmentation. There have been a number of reports on MALDI-TOF MS analysis of absolute molecular weight and end-groups for the various polymeric materials.<sup>12-18</sup> And by combining various LC methods with MALDI-TOF MS technique, both MWD and CCD information can be easily obtained for the complex polymer systems.<sup>19-24</sup> For example, Lee *et al.* carried out a precise characterization of both blocks of a PEO-*b*-PLLA diblock copolymer by LCCC combined with MALDI-TOF mass spectrometry.<sup>21</sup> They obtained fully resolved oligomeric PLLA block species at the critical condition of PEO block in the reversed-phase HPLC and successfully characterized each PLLA block species by MALDI-TOF MS. Although the combination of HPLC and MALDI-TOF MS offered high precision on the block copolymer analysis, it is a time-consuming process to fractionate the polymer by HPLC and to obtain MALDI-TOF mass spectra for all the fractions.

In this study, we attempted to fully characterize a PEO-*b*-PLLA by MALDI-TOF MS technique only. Although it is possible, in principle, if a fully resolved mass spectrum is available, it is not easy in practice since the mass peaks are significantly overlapped due to the limited resolution of MALDI-TOF MS analysis. Therefore this type of attempts has been made only for low molecular weight copolymers whose monomer molecular weights are appropriately different to minimize the peak overlap.<sup>25,26</sup> For an example, Wilczek-Vera *et al.* analyzed the MALDI-TOF mass spectra up to  $m/z \sim 4000$  of a poly( $\alpha$ -methylstyrene)-*b*-poly(4-vinylpyridine) diblock copolymers of varying poly(4-vinylpyridine) block length.<sup>26</sup> From the analysis, they could monitor the progression of the growing block chain length. The difference in the monomer molecular weight between PEO and PLLA is not as favorable for such an analysis as the case of poly( $\alpha$ -methylstyrene)-*b*-poly(4-vinylpyridine). Therefore we had to employ the isotope pattern analysis of a high-resolution MALDI-TOF mass spectrum. Isotope pattern analysis was done earlier for a low molar mass ( $M_w \cong 1,200$ ) triblock copolymer of poly(propylene oxide) and poly(ethylene oxide) of by MALDI Fourier transform ion cyclotron resonance (FTICR) MS.<sup>27</sup> In this study, we investigated a PEO-*b*-PLLA ( $M_w \cong 2,600$ ) using MALDI-TOF MS. In general, TOF method has lower resolution than FTICR, but has an advantage of less distortion in the mass spectrum over FTICR.

## Experimental

The PEO-*b*-PLLA diblock copolymer was synthesized by ring opening polymerization of L-lactide (Boehringer Ingelheim) on mono-methoxy poly(ethylene glycol) (MPEG, Aldrich) catalyzed by tin(II) bis(2-ethylhexanoate) (stannous octoate, Aldrich). The  $M_n$  and  $M_w/M_n$  of MPEG (where  $M_n$  and  $M_w$  are the number- and weight-average molecular

weight, respectively.) were determined as a 2,000 and 1.02, respectively, by MALDI-TOF MS.

In the MALDI-TOF MS experiment a Bruker REFLEX III mass spectrometer was used. The spectrometer is equipped with a nitrogen laser ( $\lambda = 337$  nm), a pulsed ion extraction, and a reflector. This instrument operated at an accelerating potential of 20 kV in reflector mode. Polymer solutions were prepared in HPLC grade THF. The matrix, trans-3-indoleacrylic acid (IAA, 99%, Aldrich) was dissolved in THF at a concentration of 15 mg/mL. A 5  $\mu$ L of the polymer solution was mixed with a 50  $\mu$ L of the matrix solution and a 1  $\mu$ L of sodium iodide solution (1 mg/mL in THF), respectively. A 0.5  $\mu$ L portion of final solution was deposited onto a sample target plate and allowed to dry in the air at room temperature.

## Results and Discussion

Figure 1(a) displays the MALDI-TOF mass spectrum of the PEO-*b*-PLLA diblock copolymer. Close examination of the spectrum reveals that the spectrum contains a number of peak envelopes, each of which consists of equally spaced peaks. The peak spacing corresponds to the mass of an eth-

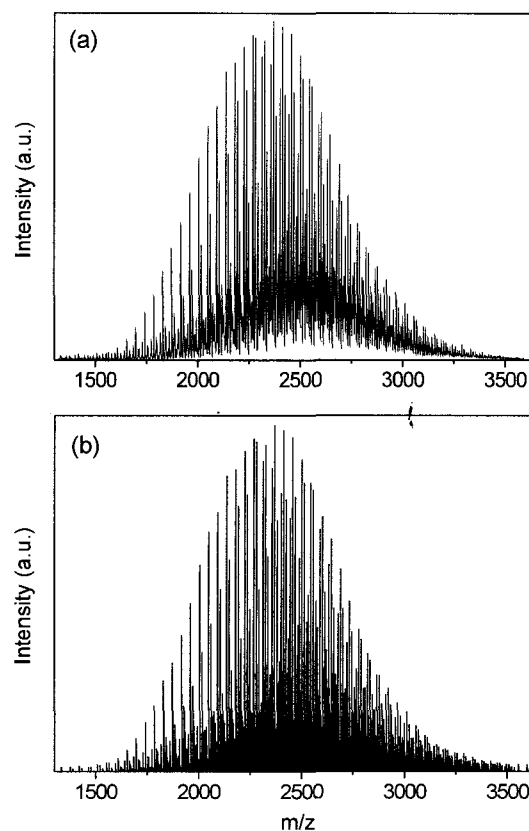


**Figure 1.** (a) MALDI-TOF mass spectrum of a PEO-*b*-PLLA diblock copolymer. Matrix: IAA, solvent: THF, salt: NaI, detection: reflection mode. (b) Reconstructed mass spectrum of the PEO-*b*-PLLA obtained from the analysis of the MALDI-TOF mass spectrum shown in Figure 1(a). Refer to the text for the details.

ylene oxide (EO) unit (formula weight: 44.05) and each envelope corresponds to the PEO-*b*-PLLA species of different PLLA block length. In principle, we can isolate the individual envelopes and obtain the complete information of the molecular weight and composition distribution of PEO-*b*-PLLA. In practice, however, the peaks are significantly overlapped due to the limited resolution of MALDI-TOF MS. Therefore this type of attempt has been made only for low molecular weight copolymers whose monomer molecular weights are appropriately apart to minimize the peak overlap. In this study, we characterize the isotope pattern of the individual peaks to extend the application to more general monomer pairs with more serious peak overlap. Figure 1(b) is the reconstructed MALDI-TOF MS spectrum from such an analysis, which is very similar to the experimental mass spectrum. The procedure to extract the necessary information is as follows.

Enlarged mass spectrum of the  $m/z$  (mass/charge) range of 2310-2365, near the maximum intensity position of the entire mass spectrum, is displayed in Figure 2(a). The spectrum spans over the mass range of one EO group difference from (LLA<sub>2</sub>, EO<sub>48</sub>) to (LLA<sub>2</sub>, EO<sub>49</sub>). Each group of 5-6 peaks represents the isotope pattern of a molecular species of

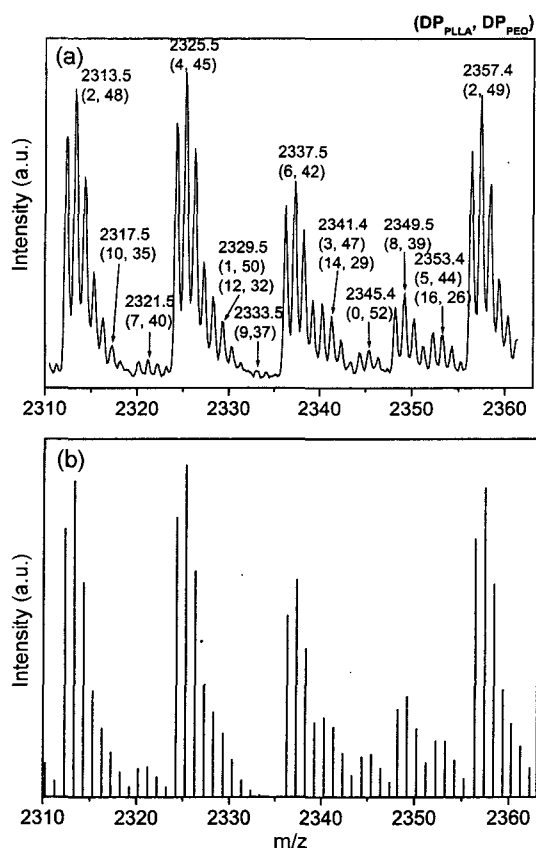


**Figure 2.** (a) Enlarged MALDI-TOF mass spectrum of the mass range from 2310 to 2365 of Figure 1 (a). (b) Reconstructed mass spectrum of the mass range from 2310 to 2365.

PEO-*b*-PLLA, which appears as a single peak in the low-resolution spectrum shown in Figure 1(a). The isotope pattern of the mass peaks can be calculated from the natural abundance of <sup>12</sup>C/<sup>13</sup>C, <sup>16</sup>O/<sup>17</sup>O/<sup>18</sup>O, and <sup>1</sup>H/<sup>2</sup>H. For example, the calculated peak intensities are shown in Table I together with the observed intensity for (LLA<sub>2</sub>, EO<sub>48</sub>) that consists of 103 carbons, 204 hydrogens, 53 oxygens, and 1 sodium ion. There are 6 peaks whose intensity is larger than 1% and the 6 peaks consist of 99.3% of the total intensity. Also we can notice that the second lowest molar mass peak shows the highest intensity. Although the isotope pattern should depend on the number of the atoms in a molecule, the second peak is always the largest in the molecular weight range shown in Figure 2(a). We labeled the number of EO and LLA units and its molar mass for the second peaks of each species in the spectrum.

In the one period of the peak pattern between (LLA<sub>2</sub>, EO<sub>48</sub>) and (LLA<sub>2</sub>, EO<sub>49</sub>) as shown in Figure 2(a), we can see the appearance of the peaks of (LLA<sub>10</sub>, EO<sub>35</sub>), (LLA<sub>7</sub>, EO<sub>40</sub>), (LLA<sub>4</sub>, EO<sub>45</sub>), (LLA<sub>1</sub>, EO<sub>50</sub> and LLA<sub>12</sub>, EO<sub>32</sub>), (LLA<sub>9</sub>, EO<sub>37</sub>), (LLA<sub>6</sub>, EO<sub>42</sub>), (LLA<sub>3</sub>, EO<sub>47</sub> and LLA<sub>14</sub>, EO<sub>29</sub>), (LLA<sub>0</sub>, EO<sub>52</sub>), (LLA<sub>8</sub>, EO<sub>39</sub>), (LLA<sub>5</sub>, EO<sub>44</sub> and LLA<sub>16</sub>, EO<sub>26</sub>) in sequence. Their molecular weights differ by about 4. Of course other combinations of LLA and EO units are also possible, but their abundance is negligible as to be discussed later. Considering the formula mass of an LLA unit (72.06) and an EO unit (44.05), the following pairs are identified to cause the peak overlap: 11 LLA (792.66) and 18 EO (792.90)  $\Delta M = 0.24$ , 8 LLA (576.48) and 13 EO (572.65)  $\Delta M = 3.83$ , and 3 LLA (216.18) and 5 EO (220.25)  $\Delta M = 4.07$ . The last two pairs with  $\Delta M \approx 4$  make the partial overlap in isotope pattern to result in the series of peak groups described above. They can be isolated by analyzing the isotope pattern with relative ease. On the other hand, the mass difference of the first pair is too small to be resolved in the mass spectrum. It means that (LLA<sub>m</sub>, EO<sub>n</sub>) peaks are almost exactly overlapped with

**Table I.** Observed and Calculated Mass of the Isotopic Content of (LLA<sub>2</sub>, EO<sub>48</sub>) and (LLA<sub>10</sub>, EO<sub>35</sub>)

Observed	Mass (amu)		Abundance		Observed
	LLA <sub>2</sub>	LLA <sub>10</sub>	LLA <sub>2</sub>	LLA <sub>10</sub>	
2312.5	2312.3		0.273		7211
2313.5	2313.3		0.327		8573
2314.5	2314.3		0.223		6067
2315.5	2315.3		0.111		3325
2316.5	2316.3	2316.1	0.044	0.278	2007
2317.5	2317.3	2317.1	0.015	0.326	1221
2318.5	2318.3	2318.2	0.004	0.221	780
		2319.2		0.109	758

( $LLA_{m+11}$ ,  $EO_{n-18}$ ) or ( $LLA_{m-11}$ ,  $EO_{n+18}$ ) and it is impossible to isolate the distribution of  $LLA_m$  from  $LLA_{m\pm 11}$  directly from the mass spectrum. However, it is possible to extract the necessary information taking advantage of the narrow molecular weight distribution of the diblock copolymer and the high abundance of PLLA blocks having even numbered LLA units since the PLLA block was polymerized by ring opening polymerization of cyclic lactide dimer.<sup>21</sup> Figure 2(b) shows the reconstructed mass spectrum from the analysis, which is very similar to the experimental mass spectrum. We will discuss on how to obtain the result.

In order to analyze the distribution of individual molecular species, we first roughly estimate the average number (highest abundance) of the EO units and LLA units in a PEO-*b*-PLLA chain from Figures 1 and 2 as ca. 50 and 4, respectively. With this information in mind, we first analyze the peaks corresponding to the species of  $LLA_2$ ,  $LLA_4$ ,  $LLA_6$ , and  $LLA_8$  that are intense and relatively easy to be isolated from the other peaks. They are supposed to be fully overlapped with  $LLA_{13}$ ,  $LLA_{15}$ ,  $LLA_{17}$ , and  $LLA_{19}$ , respectively. However the abundance of  $LLA_{13}$ ,  $LLA_{15}$ ,  $LLA_{17}$ , and  $LLA_{19}$  must be much smaller than  $LLA_2$ ,  $LLA_4$ ,  $LLA_6$ , and  $LLA_8$  since they have a much larger number of LLA units than the most abundant species ( $LLA_4$ ) and they are odd-numbered. For the even numbered, highly populated species, the second peak intensities are plotted in Figure 3(a)-(d). The second

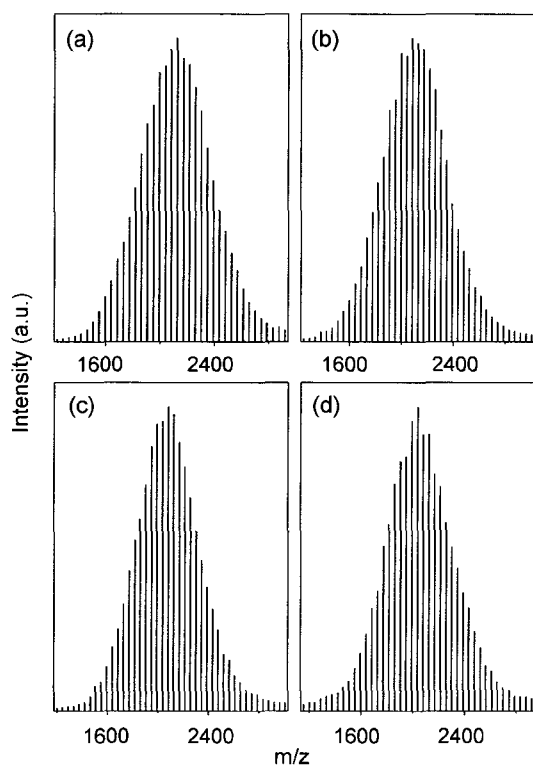


**Figure 3.** EO unit distribution at a fixed number of LLA units. (a) PEO-*b*- $LLA_2$ , (b) PEO-*b*- $LLA_4$ , (c) PEO-*b*- $LLA_6$ , and (d) PEO-*b*- $LLA_8$ .

peak was chosen because not only it is the most intense peak but also the peak is almost free from the overlap with the mass peaks of the adjacent species. Their adjacent species are  $LLA_{m+3}$  and  $LLA_{m-8}$  at  $M-4$  position and  $LLA_{m-3}$  and  $LLA_{m+8}$  at  $M+4$  position.  $LLA_{m-3}$  and  $LLA_{m+8}$  appearing at  $M+4$  position do not make any overlap with the second peak while the sixth peak of  $LLA_{m+3}$  and  $LLA_{m-8}$  overlaps with the second peak of  $LLA_m$ . As can be seen in Figure 2(a) the sixth peak intensity of  $LLA_{m+3}$  and  $LLA_{m-8}$  is much smaller than the second peak of  $LLA_m$  ( $m=2, 4, 6, 8$ ) and it is safe to extract the MW distribution of the highly abundant species from the second peak intensity directly. Their number and weight average molecular weights and their ratios ( $M_w/M_n$ ) are calculated from the distributions displayed in Figure 3(a)-(d) and summarized in Table II. In the table, the mass of PLLA block and a sodium ion are subtracted to compare the molecular weight distribution of PEO blocks only. Since the PEO-*b*-PLLA was synthesized from a PEO precursor polymer, the MW distribution of PEO block has to be identical for all the block copolymer species regardless of the PLLA block length. The plots in Figure 3 and the results in Table II show practically the identical MW distributions, which indicate that the assumptions made in the analysis scheme are acceptable for the highly abundant species within the experimental precision.

On the other hand, the other species of relatively weak intensity are not easily extracted due to the overlap with a strong adjacent species. For examples, Figure 4(a)-(c) display the molecular weight distribution curves of  $LLA_{10}$ , ( $LLA_1$  and  $LLA_{12}$ ), and ( $LLA_3$  and  $LLA_{14}$ ) obtained from the second peak intensity pattern, respectively. They have clearly distorted shapes in comparison with the distribution curves of the abundant species shown in Figure 3. In order to remove the overlapped peaks intensity we employed the following procedure.

(1) The second peak of  $LLA_m$  is overlapped with the sixth peak of  $LLA_{m-8}$  and  $LLA_{m+3}$  peaks. For an example, for  $LLA_{10}$  they are  $LLA_2$  and  $LLA_{13}$ . The contribution from  $LLA_{13}$  would be negligible compared to that of  $LLA_2$  and the sixth peak of ( $LLA_2$ ,  $EO_{48}$ ) (MW = 2,317.3, 1.49% of the total intensity of  $LLA_2$  as shown in Table I) can be regarded as the only species to contaminate the second peak of ( $LLA_{10}$ ,  $EO_{35}$ ) (MW = 2,317.1, 32.6% of the total intensity of  $LLA_{10}$  as in Table I). The peak intensity of the sixth peak

**Table II.** The Number Average ( $M_n$ ) and Weight Average ( $M_w$ ) Molecular Weight of PEO Block in the PEO-*b*- $LLA_m$  ( $m = 2, 4, 6, \text{ and } 8$ )

	$LLA_2$	$LLA_4$	$LLA_6$	$LLA_8$
$M_n$	2.10 kDa	2.08 kDa	2.07 kDa	2.04 kDa
$M_w$	2.13 kDa	2.11 kDa	2.10 kDa	2.07 kDa
$M_w/M_n$	1.01	1.01	1.01	1.01

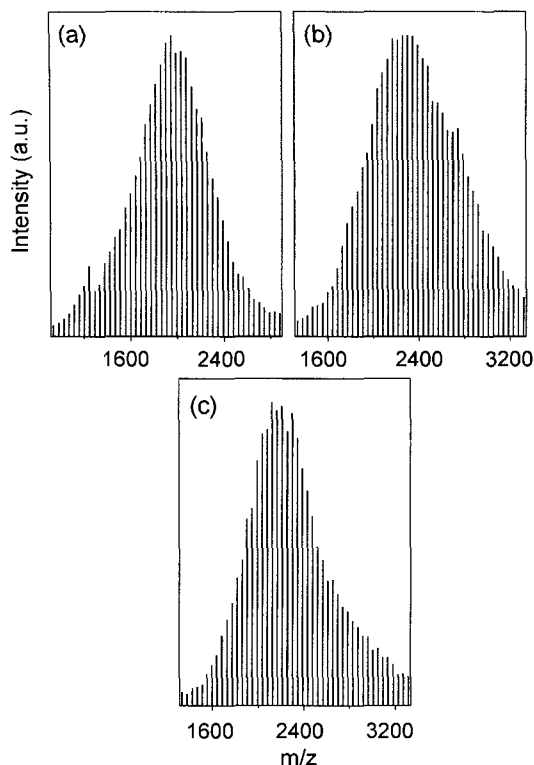


**Figure 4.** EO unit distribution at a fixed number of LLA units. (a) PEO-*b*-LLA<sub>10</sub>, (b) PEO-*b*-LLA<sub>1</sub> and PEO-*b*-LLA<sub>12</sub>, and (c) PEO-*b*-LLA<sub>3</sub> and PEO-*b*-LLA<sub>14</sub>.

of LLA<sub>2</sub> is calculated from the isotopic abundance of the two peaks (2nd peak: 0.327, 6th peak: 0.0149) and the intensity of the second peak (8573) from Table I.

$$5\text{th peak intensity of LLA}_2 = \frac{0.0149}{0.327} \times 8573 = 391$$

By subtracting the calculated intensity of the 6th peak of LLA<sub>2</sub> (391) from the peak intensity observed at MW = 2317.5 (1221) we can obtain the 2nd peak intensity of LLA<sub>10</sub> as 830. In this way, the peak overlap of LLA<sub>*m*</sub> with LLA<sub>*m*-8</sub> (and LLA<sub>*m*+3</sub>) can be removed.

(2) The other overlap problem with LLA<sub>*m*±11</sub> cannot be solved in the similar manner since their molecular weights are almost exactly overlapped. To resolve the problem, we utilize the fact that all the PEO-*b*-LLA<sub>*m*</sub> has an identical MW distribution in PEO block. In the first step, the MW distribution of PEO block is extracted from the PEO-*b*-LLA<sub>2</sub>, PEO-*b*-LLA<sub>4</sub>, PEO-*b*-LLA<sub>6</sub> block copolymers. The two-parameter Schulz-Zimm distribution, is chosen to describe the MW distribution of the PEO block, which has the following form.

$$f(n_i; t, \bar{n}) = \frac{(t\sqrt{\bar{n}})^i}{\Gamma(t)} n_i^{t-1} \exp\left(-\frac{tn_i}{\bar{n}}\right) \quad (1)$$

where  $n_i$  is the degree of polymerization (DP) of EO units,  $\bar{n}$  is the number average DP of PEO,  $t$  is a parameter related to the width of the distribution and  $\Gamma(t)$  is the gamma function. Figure 5 shows the DP distributions of PEO block in the PEO-*b*-LLA<sub>2</sub> (○), PEO-*b*-LLA<sub>4</sub> (◇), PEO-*b*-LLA<sub>6</sub> (□) block copolymers obtained from the MALDI-TOF MS spectra shown in Figure 3. As expected, they have very similar distributions and the fitting to Eq. 1 (solid line) yielded  $\bar{n} = 46.7$  and  $t = 61.0$ .

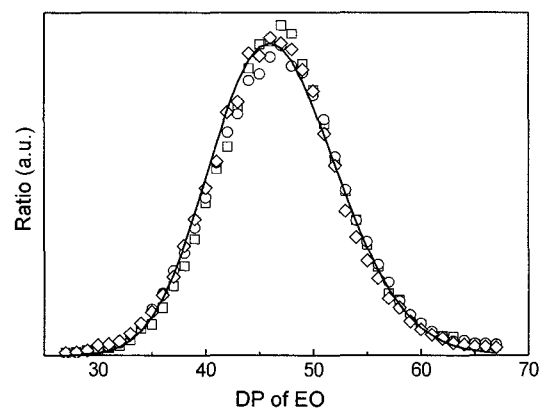
From the model, the overlapped peaks of (LLA<sub>*m*</sub>, EO<sub>*n*</sub>) and (LLA<sub>*m*+11</sub>, EO<sub>*n*-18</sub>) can be separated by fitting the distribution to the following bimodal distribution.

$$f(n_i) = r_m f(n_i) + r_{m+11} f(n_i - 18) \quad (2)$$

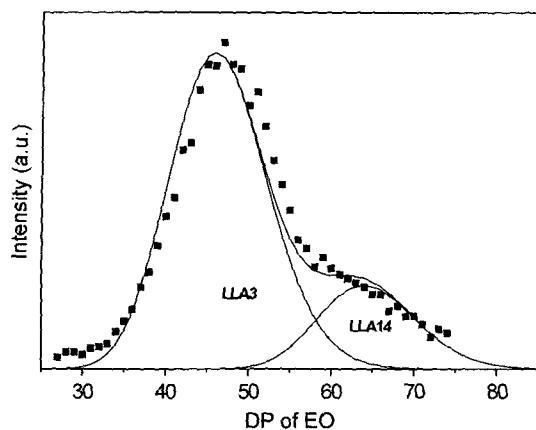
where  $r_m$  is the relative abundance of PEO-*b*-LLA<sub>*m*</sub>. Figure 6 shows an example of such analyses for the overlapped distribution of LLA<sub>3</sub> and LLA<sub>14</sub>. The fitting quality cannot be said excellent but acceptable to extract the relative contribution of the two species. The fitting quality could be improved by floating  $\bar{n}$  and the separation of two peaks, but we fixed them as 46.7 and 18 since it constitutes the basis of this analysis scheme.

Figure 2(b) is the reconstructed spectrum for the *m/z* range of 2310-2365 from the analysis procedure described above. It is very similar to the measured mass spectrum displayed in Figure 2(a). In this way, the whole mass spectrum was reconstructed as shown in Figure 1(b), which appears almost indistinguishable from the measured spectrum. Figure 7 displays a 2D distribution of EO and LLA units in the PEO-*b*-PLLA obtained from the analysis described above. As expected, the diblock copolymer shows a highest population at (LLA<sub>4</sub>, EO<sub>45</sub>) and the species with even number of LLA units show much higher abundance than the odd-numbered ones.

In summary, we characterized the molecular weight and composition distribution of a PEO-*b*-PLLA diblock copolymer



**Figure 5.** Fitting EO unit distribution to the Schulz-Zimm distribution function (Eq. 1): PEO-*b*-LLA<sub>2</sub> (○), PEO-*b*-LLA<sub>4</sub> (◇), PEO-*b*-LLA<sub>6</sub> (□) and the fit result (solid line).



**Figure 6.** Fitting overlapped EO unit distribution of PEO-*b*-LLA<sub>3</sub> and PEO-*b*-LLA<sub>14</sub> to the two Schulz-Zimm distribution functions that are apart by 18 EO units (Eq. 2). The filled squares are the experimental data and the lines are the isolated distributions of PEO-*b*-LLA<sub>3</sub> and PEO-*b*-LLA<sub>14</sub> from the fit. Abscissa stands for the degree of polymerization of the PEO block in PEO-*b*-LLA<sub>3</sub>. For PEO-*b*-LLA<sub>14</sub>, 18 needs to be subtracted.

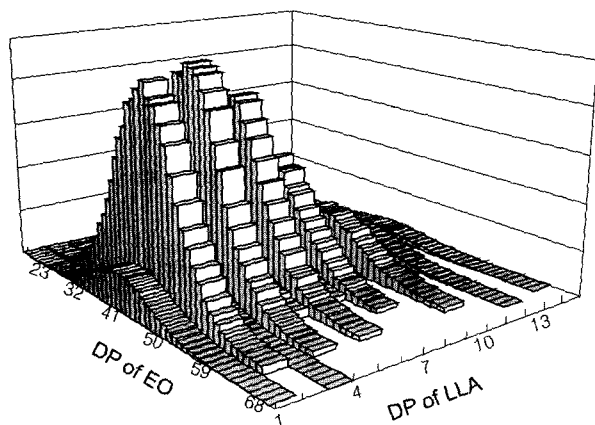


**Figure 7.** Distribution map of EO and LLA units in the PEO-*b*-PLLA.

by MALDI-TOF MS only. From a mass spectrum with a practically available mass resolution, a full characterization of the block copolymer was possible utilizing the isotope pattern analysis. Although the application of this type of analysis has been limited to relatively low molecular weight polymers, it can be very useful if such low molecular weight polymers have a practical use as exemplified by the PEO-*b*-PLLA in this study. Such an isotope pattern analysis can be expedited by computer programming, which is the most attractive feature of this method over HPLC separation.

**Acknowledgements.** This study is supported in part by research grants to T.C. from KOSEF (Center for Integrated Molecular Systems) and BK21 program. D.S. Lee acknowl-

edges the support from KOSEF (Center for Advanced Functional Polymers).

## References

- (1) B. Jeong, Y. H. Bae, D. S. Lee, and S. W. Kim, *Nature*, **388**, 860 (1997).
- (2) S. Tanodekaew, R. Pannu, F. Heatley, D. Attwood, and C. Booth, *Macromol. Chem. Phys.*, **198**, 927 (1997).
- (3) H. T. Lee and D. S. Lee, *Macromol. Res.*, **10**, 359 (2002).
- (4) S. H. Lee, S. H. Kim, Y. H. Kim, and Y.-K. Han, *Macromol. Res.*, **10**, 85 (2002).
- (5) G. Glöckner, *Gradient HPLC of Copolymers and Chromatographic Cross-Fractionation*, Springer-Verlag, Berlin, 1992.
- (6) H. Pasch and B. Trathnigg, *HPLC of Polymers*, Springer-Verlag, Berlin, 1997.
- (7) D. Berek, *Prog. Polym. Sci.*, **25**, 873 (2000).
- (8) R. Murphy, M. Schure, and J. Foley, *Anal. Chem.*, **70**, 4353 (1998).
- (9) P. Jandera, M. Holcapek, and L. Kolarova, *J. Chromatogr. A*, **869**, 65 (2000).
- (10) S. Park, D. Cho, J. Ryu, K. Kwon, W. Lee, and T. Chang, *Macromolecules*, **35**, 5974 (2002).
- (11) B. G. Belenkii, E. S. Gankina, M. B. Tennikov, and L. Z. Vilenchik, *J. Chromatogr.*, **147**, 99 (1978).
- (12) A. M. Belu, J. M. DeSimone, R. W. Linton, G. W. Lange, and R. M. Friedman, *J. Am. Soc. Mass Spectrom.*, **7**, 11 (1996).
- (13) A. T. Jackson, H. T. Yates, J. H. Scrivens, M. R. Green, and R. H. Bateman, *J. Am. Soc. Mass Spectrom.*, **8**, 1206 (1997).
- (14) D. C. Schriemer, R. M. Whittal, and L. Li, *Macromolecules*, **30**, 1955 (1997).
- (15) M. W. F. Nielen, *Mass. Spec. Rev.*, **18**, 309 (1999).
- (16) Y. C. Shin, K. Y. Choi, M. Y. Jin, S. K. Hong, D. Cho, T. Chang, and M. Ree, *Korea Polym. J.*, **9**, 100 (2001).
- (17) D. Cho, S. Park, K. Kwon, and T. Chang, *Macromolecules*, **34**, 7570 (2001).
- (18) S. Park, D. Cho, J. Ryu, K. Kwon, T. Chang, and J. Park, *J. Chromatogr. A*, **958**, 183 (2002).
- (19) M. S. Montaudo, C. Puglisi, F. Samperi, and G. Montaudo, *Macromolecules*, **31**, 3839 (1998).
- (20) M. S. Montaudo and G. Montaudo, *Macromolecules*, **32**, 7015 (1999).
- (21) H. Lee, W. Lee, T. Chang, S. Choi, D. S. Lee, H. Ji, W. K. Nonidez, and J. W. Mays, *Macromolecules*, **32**, 4143 (1999).
- (22) H. Lee, T. Chang, D. S. Lee, M. S. Shim, H. Ji, W. K. Nonidez, and J. W. Mays, *Anal. Chem.*, **73**, 1726 (2001).
- (23) D. Cho, S. Park, T. Chang, K. Ute, I. Fukuda, and T. Kitayama, *Anal. Chem.*, **74**, 1928 (2002).
- (24) D. Cho, J. Hong, S. Park, and T. Chang, *J. Chromatogr. A*, **986**, 199 (2003).
- (25) G. Wilczek-Vera, P. O. Danis, and A. Eisenberg, *Macromolecules*, **29**, 4036 (1996).
- (26) G. Wilczek-Vera, Y. Yu, K. Waddell, P. O. Danis, and A. Eisenberg, *Rapid Commun. Mass Spectrom.*, **13**, 764 (1999).
- (27) G. J. van Rooij, M. C. Duursma, C. G. de Koster, R. M. A. Heeren, J. J. Boon, P. J. W. Schuyf, and E. R. E. van der Hage, *Anal. Chem.*, **70**, 843 (1998).